An assessment of regional sea ice predictability in the Arctic ocean

Rubén Cruz-García*, Virginie Guemas, Matthieu Chevallier, François Massonnet
*Barcelona Supercomputing Center (BSC-ES), C/ Jordi Girona 29, 08034, Barcelona, Spain.
Email: ruben.cruzgarcia@bsc.es

Abstract*—Arctic sea ice plays a central role in the Earth's climate. Changes in the sea ice on seasonal-to-interannual timescales impact ecosystems, populations and a growing number of stakeholders. A prerequisite for achieving better sea ice predictions is a better understanding of the underlying mechanisms of sea ice predictability. Previous studies have shown that sea ice predictability depends on the predictand (area, extent, volume), region, and the initial and target dates. Here we investigate seasonal-to-interannual sea ice predictability in so-called "perfect model" 3-year-long experiments run with the EC-Earth 2.3 climate model initialized in early July. Consistent with previous studies, robust mechanisms for reemergence are highlighted, i.e. increases in the autocorrelation of sea ice properties after an initial loss. We find that Arctic regions can be classified according to three distinct regimes. The central Arctic drives most of the pan-Arctic sea ice volume persistence. In peripheral seas, we find trivial predictability for the sea ice area in winter but low predictability throughout the rest of the year, due to the particularly unpredictable sea ice edge location. The Labrador Sea stands out among the considered regions, with sea ice predictability extending up to 1.5 years if the oceanic conditions upstream are known.

I. Methodology

We used a 300-year long present day control experiment under perpetual 2005 forcing (*ControlRun*). This single-member experiment provides the initial conditions used to perform a set of idealized climate prediction experiments initialized from July 1st (*IdealPred*). The predictions last 3 years and consist of 8 members, each of them with slightly different perturbations of the initial sea surface temperature (SST; 10^{-4} K magnitude).

For evaluating the predictability we consider the **prognostic potential predictability** (**PPP** hereafter). It compares the ensemble spread with an estimation of the amplitude of the natural variability of the system based on the standard deviation of the control simulation, and addresses the initial value predictability. A PPP value of 1 would mean that we have a perfectly predictable system. Predictability is estimated both in a prognostic (PPP) and diagnostic (lagged *ControlRun* properties) way. The **prognostic approach** suffers from insufficient sampling, in contrast with the long control simulation, that can be used to supply that problem.

Breaking down the **analysis into sectors** is essential since the pan-Arctic sea ice extent (SIE), area (SIA) and volume (SIV) integrate a large variety of regions which are regulated by different physical mechanisms. Thus, predictability was investigated for each Arctic sea (Fig. 1). Lagged SIE autocorrelation for each month against lead time shows the **September to September** correlation reemergence (**leadtime 12**), consistent with Blanchard et al. (AMS, 2011) mechanism from one summer to the next. The **melt-to-freeze** mechanism is present in July (**leadtime 3**). The SIV memory regime is characterized by its vast persistence for all start months.

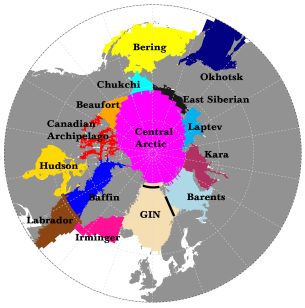

Figure 1: Map of the Arctic seas as defined in this study. The black lines indicate the sections used for the calculation of the Atlantic heat transport into the Arctic (Fram Strait plus Barents Sea Opening). The GIN region is formed by the Greenland, Icelandic and Norwegian seas.

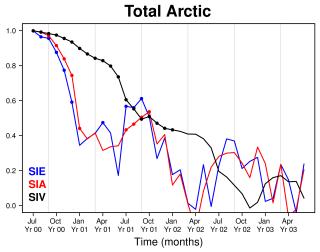

Figure 2: Potential predictability of the total Arctic SIE (blue), SIA (red) and SIV (black) measured with the PPP of *IdealPred* using the natural variability of *ControlRun* as a reference. Dots indicate significant values at the 95 % level, estimated by Fisher's test. September and March are marked by thin gray vertical lines.

II. Pan-Arctic sea ice

The **melt-to-freeze** mode is not only present in the lagged correlations (not shown), but it is also a feature in the predictions initialized in July (Fig. 2).

The **long SIV predictability** agrees with the lagged correlations (not shown). This persistence comes almost entirely from the central Arctic SIV memory, as can be checked when comparing the lagged correlation of central and pan-Arctic SIV (Fig. 2; blue and black lines).

Summer-to-summer memory reemergence has its origin in the summer SIT memory (from the central Arctic). Over three continuous years, the **central SIV and SIE are synchronously correlated in September** (not shown).

III. Regional Arctic sea ice

In the Barents Sea, peaks of reemergence occur the second and third summer (not shown). Synchronous correlation between the SST and the SIE (Fig. 3, red line) reveals that **SST** is a **source of SIE predictability** in December. Correlation between the gridpoint SST in December and SIE from December to February confirms this timeseries. The SST during the previous spring also provides predictability to the December SIE (not shown).

The PPP of the SIE in the interior basins (e.g. the Canadian Archipelago; Fig. 4) saturates in winter because of the **extremely**

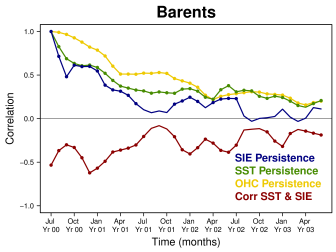

Figure 3: The persistence of the SIE (blue), the SST (green), OHC (0-300 m depth, yellow) for the Barents Sea. In red, the synchronous correlation between the SST and the SIE. Correlations were calculated using the *ControlRun* during the three subsequent years. The dots represent significant values at the 95% level as estimated from a one-sided student-T distribution.

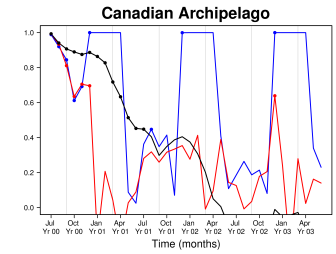

Figure 4: As Fig. 2 for the Canadian Archipelago.

low sea ice variability. SIA PPP differs from SIE signal because its variability is larger in winter, with non-fully covered ice regions. In most of central regions SIV is potentially predictable up to one year before.

Backward trajectories from the **Labrador Sea** reveal that the **water masses origin is the Irminger Sea**, and the North Atlantic Ocean in a longer term (Fig. 5a-b). The **Irminger Sea SST and ocean heat content (OHC)** at the moment of the initialization and the Labrador Sea SIE are significantly anticorrelated from February to July the two first years, matching exactly the time when the PPP reemergence in the Labrador Sea occurs (Fig. 5c).

IV. Conclusions

- Pan–Arctic SIE experiences melt-to-freeze reemergence both in the prognostic ensemble potential predictability and in the control run lagged correlations. The SIV shows greater predictability, attributable to the long-lasting persistence of the SIT in the central Arctic SIT.
- The summer-to-summer reemergence of the PPP of pan-Arctic SIE is due to the persistence of SIT anomalies in the central Arctic.
- In the peripheral seas of the Atlantic Sector, significantly high PPP values over 1 year are driven by the persistence of local oceanic thermal anomalies (SST and OHC).
- In the Labrador Sea, which is ice-free in July, the PPP peaks between January and April as result of the advection of ocean temperature anomalies from the Irminger Sea and the Eastern North Atlantic Ocean.
- In the interior Arctic seas, winter SIE potential predictability is trivial due to complete ice coverage. No significant predictability was found for the SIA. In contrast, the SIV has a longer predictability in this set of seas as a result of the long SIT persistence.

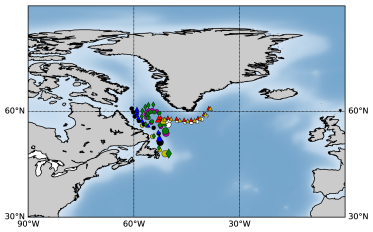

(a)

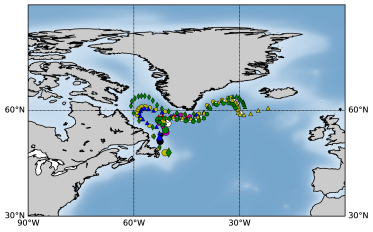

(b)

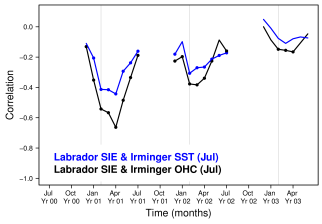

(c)

Figure 5: Map of the backward trajectories followed by water masses travelling from different locations in the Labrador Sea from **(a)** the first and **(b)** the second February until the first July. Each lead time is marked with a dot, while the initial positions (corresponding February) are marked with bigger dots. **(c)** Correlation between the Labrador Sea SIE and the Irminger SST (in blue) and the Irminger OHC (0-300 m depth; in black) the first July for the *ControlRun* during the three following years. The dots represent the significant values at the 95% level estimated from a one-sided student-T distribution. The vertical grey lines represent the months of February. The SST and OHC were integrated for the corresponding area in Fig. 1.

Rubén Cruz-García. Rubén studied his bachelor in Environmental Sciences at University of Murcia, where he discovered his passion for investigating the climate change. After that, he began a Master degree in Geophysics and Meteorology at University of Granada. He started his PhD project in the Climate Prediction Group at the Earth Sciences Department of the Barcelona Supercomputing Center in October 2015. His work focuses on assessing the predictability and the prediction skill of the Arctic sea ice conditions at the regional scale using two state-of-the-art dynamical models, EC-Earth and CNRM-CM.